

Numerical Analysis of Hypersonic Combustion without Cavity Based Injection with Finite Rate Chemistry Model

A.P. Singh¹, K.M.Pandey², Arun Burman¹, Mohit Sharma³, Navneet Tyagi³

¹Department of Mechanical Engineering, Bharat Institute of Technology, Meerut, UP, India, hello2apsingh@gmail.com

²Department of Mechanical Engineering, National Institute of Technology, Silchar Assam, India, kmpandey2001@yahoo.com

³Department of Mechanical Engineering, Bharat Institute of Technology, Meerut, UP, India



Abstract : In this part of the investigation, flow-field properties of hydrogen jets injected into a hypersonic flow are reported. The combustor has a single fuel injection parallel to the main flow from the base. The numerical simulation has been done with finite rate chemistry model using K- ϵ turbulence model. The results obtained through the numerical simulation of the cavity based fuel injectors are presented. The main issue in supersonic combustion is proper mixing within short burst of time. The result shows the better mixing of fuel and the flame speed increases almost linearly. The stagnation temperature in the combustion reaches up to 2510 k.

Key words: Hypersonic combustion, Mach number, K- ϵ turbulence model, finite rate, flame speed

INTRODUCTION

Supersonic combustion is the key enabling technology for sustained hypersonic flights. In scramjet engines of current interest, the combustor length is typically of the order of 1 m, and the residence time of the mixture is of the order of milliseconds. Due to the high supersonic flow speed in the combustion chamber, problems arise in the mixing of the reactants, flame anchoring and stability and completion of combustion within the limited combustor length. The flow field in the scramjet combustor is highly complex. It is shown that when the flight speed is low, the kinetic energy of the air is not enough to be used for the optimal compression. Further compression by machines is needed in order to obtain a higher efficiency. For example, a turbojet employs a turbine machine for further compression. When the flight speed is higher than a certain value, the air flow entering a combustor will remain to be supersonic after the optimal compression. With a further compression (i. e. deceleration), the efficiency of the engine will decrease. Therefore the combustion has to take place under the supersonic flow condition. This kind of air-breathing engine, which works under hypersonic flight condition, is called the supersonic combustion ramjet (Scramjet). The term of "supersonic combustion" applied here means the combustion in a supersonic flow. The efficiency of heat supply to the combustion chamber based on the analysis of literature data on combustion processes in a confined high-velocity and high-temperature flow for known initial parameters is considered. This was given by Tretyakov[2007]. The process efficiency is characterized by the combustion completeness and total pressure losses. The main attention is paid to the local intensity of heat release, which determines, together with the duct geometry, techniques for flame initiation and stabilization, injection techniques and quality of mixing the fuel with oxidizer, the gas-dynamic flow regime. The study of supersonic

combustion of hydrogen has been conducted by Shigeru Aso et al. [2005] using a reflected-type shock tunnel which generated a stable supersonic air flow of Mach number of 2 with the total temperature of 2800K and the total pressure of 0.35 MPa. He concluded that The Schlieren images show that the increase of injection pressure generated strong bow shock, resulting in the pressure losses.

Supersonic combustion data obtained at the low static temperatures appropriate for an efficient scramjet engine are reviewed by T.Cain and C. Walton[2007]. Attention is focused at the methods by which the fuel was ignited and combustion maintained. This is particularly common for supersonic combustion experiments and many examples are found in the literature of experiments conducted with inlet temperatures much higher than practical in flight. There is a good reason for this: it is difficult to sustain a hydrogen or hydrocarbon flame in a low temperature supersonic flow. A well designed combustor makes this possible; a less effective combustor can be made to function simply by elevating the static temperature until spontaneous ignition is achieved.

Low combustor entry temperature is desirable/essential due to intake and nozzle limitations.

This paper aims in particular at the application of scalar and joint scalar-velocity-turbulent frequency PDF (probability density functions) methods to supersonic combustion done by P. Gerlinger et al[2003]. Supersonic combustion has the potential of providing propulsion systems for a new generation of air breathing space transportation vehicles. Accuracy is an all-important issue. Supersonic combustion is commonly considered as one of the most demanding applications of current CFD tools.. However, rapid ignitions as well as fast and complete combustion are vital to reduce hardware length and weight. Therefore, hydrogen is the fuel of choice owing to its short ignition delay and, in view of structural mechanics, because of its efficiency in cooling. As a last point it may be concluded that more high-quality experimental data are indispensable for further evaluation of high speed combustion models.

A numerical study of mixing and combustion enhancement has been performed by Peter Gerlinger et al[2008] for a Mach 2 . Due to the extremely short residence time of the air in supersonic combustors, an efficient (rapid and with small losses in total pressure) fuel/air mixing is hard to achieve. K. Kumaran &V.Babu [2009] investigates the effect of chemistry models on the predictions of supersonic combustion of hydrogen in a model combustor. The calculations show that multi step chemistry predicts higher and wider spread heat release than what is predicted by single step chemistry. In addition, it is also shown that multi step chemistry predicts intricate details of the combustion process such as the ignition distance and induction distance. a

detailed chemistry model with 37 reactions and 9 species was used and the results from these calculations were compared with those obtained using single step chemistry.

However, the prediction of the myriad details of the heat release/ignition delay, which offer insights into the combustion process, demands a comprehensive chemistry model as demonstrated in this work.

A numerical study of atomization, i.e. breakup of a high speed jet and spray formation, is presented by Zhiliang Xu & Wohno Ohz [2006] using the Front Tracking method in 2D. The high speed flow in the nozzle gives rise to cavitation, i.e. a mixed liquid-vapor region.

A Lagrangian model of turbulent combustion in high speed flows has been used in conjunction with an efficient RANS-AMA strategy to simulate both non-reactive and reactive turbulent supersonic co-flowing jets. Liquid hydrocarbon supersonic combustion has been experimentally investigated by C. GRUENIG & F. Mayinger. Kerosene was burnt in a steady, vitiated Mach 2.15 - air flow of a model scramjet combustor. The fuel is injected into the supersonic air stream by means of pylons. By the addition of small amounts of hydrogen to the kerosene the liquid fuel jet is dispersed and a fine spray produced. However, this additional fuel jet dispersion is not necessary for the supersonic combustion if the fuel is injected normally into the cross flow. Combustor ignition behavior, the air stream temperature can be reduced below the combustor ignition level T_{min} once the combustor has ignited. Below $T_{flame-out}$ the time scale ratio $t_{ignition}/t_{residence}$ reaches its unstable regime again and the flame extinguishes.

MATERIAL AND METHODS PHYSICAL MODEL

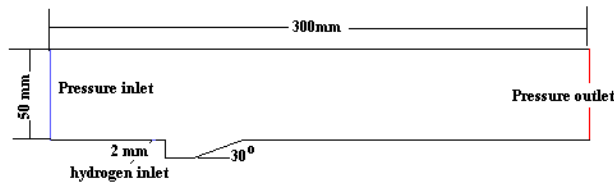


Figure 1 Sketch of the hypersonic combustor with cavity based injection.

Governing equations

The governing equations for a general coordinate comprise the mass conservation equation, the full Navier-Stokes equation, energy and species transport equations for a chemically reacting gas composed of N species as follows by poinot [2005]

$$\frac{\partial \bar{Q}}{\partial t} + \frac{\partial (\bar{F} - \bar{F}_v)}{\partial \xi} + \frac{\partial (\bar{G} - \bar{G}_v)}{\partial \eta} = \bar{S} \quad (34)$$

Where the conservative vector is \bar{Q} and the convection and viscous terms in the ξ and η

direction are \bar{F} , \bar{G} and \bar{F}_v , \bar{G}_v respectively and defined as below. The source term for chemical reaction is \bar{S} .

$$\bar{Q} = \frac{1}{J} \bar{Q} = \frac{1}{J} \begin{pmatrix} \rho \\ \rho u \\ \rho v \\ \rho e_i \\ \rho Y_i \end{pmatrix}, \quad \bar{S} = \frac{1}{J} \bar{S} = \frac{1}{J} \begin{pmatrix} 0 \\ 0 \\ 0 \\ 0 \\ \dot{\omega}_i \end{pmatrix},$$

$$\bar{F} = \frac{1}{J} (\xi_x F + \eta_x G) = \frac{1}{J} \begin{pmatrix} \rho u \\ \rho u^2 + \xi_x P \\ \rho v u + \xi_y P \\ h \rho u \\ Y_i \rho u \end{pmatrix},$$

$$\bar{G} = \frac{1}{J} (\xi_y F + \eta_y G) = \frac{1}{J} \begin{pmatrix} \rho v \\ \rho u v + \eta_x P \\ \rho v^2 + \eta_y P \\ h \rho v \\ Y_i \rho v \end{pmatrix},$$

$$\bar{F}_v = \frac{1}{J} (\xi_x F_v + \eta_x G_v), \quad \bar{G}_v = \frac{1}{J} (\xi_y F_v + \eta_y G_v),$$

$$F_v = \begin{pmatrix} 0 \\ \tau_{xx} \\ \tau_{xy} \\ u \tau_{xx} + v \tau_{xy} - q_x \\ \rho D_i \frac{\partial Y_i}{\partial x} \end{pmatrix}, \quad G_v = \begin{pmatrix} 0 \\ \tau_{xy} \\ \tau_{yy} \\ u \tau_{xy} + v \tau_{yy} - q_y \\ \rho D_i \frac{\partial Y_i}{\partial y} \end{pmatrix}. \quad (1)$$

The shear stress and heat flux in viscous terms may be denoted by the following equations

$$\tau_{xx} = \frac{\mu}{\text{Re}_\infty} \left(\frac{4}{3} \frac{\partial u}{\partial x} - \frac{2}{3} \frac{\partial v}{\partial y} \right)$$

$$\tau_{yy} = \frac{\mu}{\text{Re}_\infty} \left(\frac{4}{3} \frac{\partial v}{\partial y} - \frac{2}{3} \frac{\partial u}{\partial x} \right), \quad \tau_{xy} = \frac{\mu}{\text{Re}_\infty} \left(\frac{\partial u}{\partial x} + \frac{\partial v}{\partial y} \right), \quad (2)$$

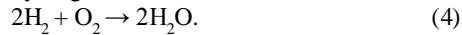
$$q_x = -\frac{1}{\text{Re}_\infty P_r (\gamma - 1)} K \frac{\partial T}{\partial x} - \frac{1}{\text{Re}_\infty \text{Sc}_\infty} \rho \sum_{i=1}^{N_s-1} h_i D_i \frac{\partial Y_i}{\partial x},$$

$$q_y = -\frac{1}{\text{Re}_\infty P_r (\gamma - 1)} K \frac{\partial T}{\partial y} - \frac{1}{\text{Re}_\infty \text{Sc}_\infty} \rho \sum_{i=1}^{N_s-1} h_i D_i \frac{\partial Y_i}{\partial y}, \quad (3)$$

Where u and v are the velocity components in the x and y directions. Symbols Re_∞ , Pr , K , γ , and Sc_∞ are the Reynolds number, Prandtl number, thermal conductivity, specific heat ratio, and Schmidt number, respectively. D_i , h_i , and Y_i are diffusion coefficient, enthalpy and mass fraction for species i .

Reaction model

The instantaneous reaction model assumes that a single chemical reaction occurs and proceeds instantaneously to completion. The reaction used for the Scramjet was the hydrogen-water reaction:



The equilibrium model

The equilibrium model requires the specification of all the chemical species that might exist in the reacting mixture. No specific reactions need to be specified. This reaction model calculates the species concentrations at its equilibrium condition. The species specified for the reaction mixture were: H_2 , O_2 , N_2 , H_2O , OH , O and NO .

The multi-step finite rate reaction model uses chemical rate equations to model any number reaction occurring in the system. The reaction rates are calculated using the Arrhenius equation:

$$k = A_p T^n e^{(-E_n/RT)} \quad (5)$$

where: k is the reaction rate coefficient A_p is the pre-exponential constant E_n/R is the activation temperature n is the temperature exponent

K-ε Turbulence model

Modified k-ε model called Renormalization Group (RNG) is proposed by Yakhot et al. [1992], which systematically removes all the small scale of turbulence motion from the governing equation by expressing their effect in terms of large scales and a modified viscosity.

$$\frac{\partial(\rho\kappa)}{\partial t} + \nabla \cdot (\rho\kappa u) = \text{div} [a_k \mu_{eff} \text{grad}\kappa] + H_k \quad (6)$$

$$\frac{\partial(\rho\varepsilon)}{\partial t} + \text{div}(\rho\varepsilon U) = \text{div} [a_\varepsilon \mu_{eff} \text{grad}\varepsilon] + H_\varepsilon \quad (7)$$

Here the turbulence source term are defined as

$$H_k = 2\mu_t E_{ij} - \rho\varepsilon \quad \text{and} \\ H_\varepsilon = C_{1\varepsilon}^* \frac{\varepsilon}{\kappa} 2\mu_t E_{ij} \cdot E_{ij} - C_{2\varepsilon} \rho \frac{\varepsilon^2}{\kappa} \quad (8)$$

Turbulence viscosity is defined as

$$\mu_t = \rho C_\mu \frac{\kappa^2}{\varepsilon} \quad (9)$$

Closure coefficient are evaluated as

$$C_\mu = 0.0845, \quad \alpha_\kappa = \alpha_\varepsilon = 1.39, \quad C_{1\varepsilon} = 1.42, \\ C_{2\varepsilon} = 1.68$$

$$\eta = \sqrt{\left(2E_{ij} \cdot E_{ij}\right)^{\frac{\kappa}{\varepsilon}}} \quad \text{and} \quad C_{1\varepsilon}^* = C_{1\varepsilon} - \frac{\eta(1-\eta/\eta_0)}{1+\beta\eta^3}$$

$$\eta_0 = 4.377, \quad \beta = 0.012$$

Value of constant β is adjustable which is found from near the wall turbulence data.

Degree of Mixing and Mixing Efficiency

The jet penetration is a global measure that promotes fuel-air mixing. In fact, the jet-mixture fraction distribution is of more interest because it helps identify the regions where sufficient mixing has occurred to enable the initiation and propagation of chemical reactions. In a simple, two-component system, the concentration is defined by the mass-flow ratio. A mixedness parameter was defined by Liscinsky et al. [1995] as

$$U = \frac{c_{var}}{c_{avg}(1-c_{avg})} \quad (10)$$

Where c_{var} is a spatial concentration variance defined as

$$c_{var} = \frac{1}{n} \sum_{i=1}^n (\bar{c}_i - c_{avg})^2$$

\bar{c}_i is the time-averaged concentration at any given location, and the average concentration c_{avg} determined from the global mass flows of the jet and the airstream as $c_{avg} = [m_{jet}/m_{jet} + m_{air}]$. This normalization by the product $c_{avg}(1-c_{avg})$ removes the dependence on the jet-to-air mass-flow ratio.

The concentration variation described by the mixedness parameter U indicates the degree to which the two components in the system are present within a given volume in the flow. In a sense, this parameter is not unlike the non-uniformity mass-fraction parameter introduced by Kopchenov and Lomkov [147], defined as

$$D = \frac{\int_A \rho u (c - \bar{c})^2 dA}{\bar{c}^2 \int_A \rho u dA} \quad (11)$$

Where D is the non-uniformity mass fraction; ρ , u , and c are the local density, velocity, and concentration, respectively; A is the cross section of the axial station where mixing is

evaluated; and \bar{c} is the mass-averaged concentration in the cross section. A value of $D = 0$ indicates full uniformity and $D = 1$ indicates complete lack of injectant. The first parameter, U , is a local concentration measurement whereas the second, D , offers a cross-sectional measure.

The degree of mixedness based on concentration decay, for this purpose it is useful to relate the mixing parameter to the stoichiometric ratio. This suggests the use of a mixing-efficiency parameter, which indicates the fraction of

the reactant that would react if brought to chemical equilibrium with the air. The fraction of the reactant refers to the least-available reactant, air, or fuel, depending on whether the mixture is lean or rich; in fuel-lean regions, the mixing-efficiency parameter represents the fraction of fuel, and in fuel-rich regions the mixing efficiency refers to the fraction of air. The fuel fraction defined in this fashion takes the following values,

$$\alpha_{react} = \begin{cases} \alpha & \alpha \leq \alpha_{stoic} \\ \alpha(1-\alpha)/(1-\alpha_{stoic}) & \text{For } \alpha > \alpha_{stoic} \end{cases} \quad (12)$$

where α is the fuel mass fraction, α_{react} is the fuel fraction mixed in a proportion that can react, and α_{stoic} is the fuel stoichiometric mass fraction. The mixing efficiency is then defined as

$$\eta_m = \frac{m_{fuel,mixed}}{m_{fuel,total}} = \frac{\int \alpha_{react} \rho u dA}{\int \alpha \rho u dA} \quad (13)$$

Where $m_{fuel, mixed}$ is the mixed fuel mass flow and $m_{fuel, total}$ is the total fuel flow rate. Equation (4.7) thus defines a mixing efficiency in a cross section, with $m = 1$ indicating a perfectly mixed system. In this case the maximum value of fuel fraction must remain less than or equal to the stoichiometric ratio.

Combustion Efficiency and Total Pressure Loss

Combustion efficiency is measure of the degree of the completeness of combustion, combustion efficiency at given $x = \text{constant}$ section is measure of how much of the fuel injected upstream has been consumed at that station and defined as;

$$\eta_c = \frac{m_{fuel,in} - m_{fuel,x}}{m_{fuel,in}} = 1 - \frac{\int \alpha \rho u dA}{\sum \dot{m}_{fuel,in}} \quad (14)$$

Where $\dot{m}_{fuel,in}$ is local fuel mass flow rate.

RESULT AND DISCUSSION

The most significant technological problem for implementation of hypersonic air breathing propulsion is the process of mixing the injected fuel with the free stream oxidant. A particularly difficult challenge is presented for combination of fuel and air at very high Mach numbers and high enthalpy since combustion proceeds at supersonic velocities. Extremely short combustor residence times coupled with the requirement of limited combustor length necessitates some form of mixing augmentation over that provided by stream wise shear alone. Figure 2 shows the contours of Mach number at 5.14, the deflection of path lines clearly shows the oblique shock wave from the upstream face of injection. Near the injector the flow is subsonic in separated region as it can be clearly visualized in contour of Mach number. While in the recalculated zone the Mach number is around 3.10. The small instantaneous fluctuations of the bow shock are observed to average into a smoother and

slightly thicker one. Figure 3, Static pressure for the reacting flow on the lower and upper wall is quite different. The pressure rise due to the combustion is not very high on account of global equivalence ratio being quite low. Within the inlet the shock-wave-boundary-layer interactions play a significant role. When sufficiently strong, these shock waves impinge on the boundary layers that are sensitized by adverse pressure gradients caused by a pressure raise in the combustion chamber, leading to flow separations and producing several adverse effects on the inlet operation. Furthermore, the local boundary-layer distortion generates a new structure of shock waves and modifies the inlet-flow structure.

Flame holding requires achieving a balance between the flame propagation speed and the fluid velocity. Because the fluid velocity exceeds the flame speed in supersonic combustion applications, the flame holding issue is solved by the generation of some sort of recirculation region that ensures sufficient residence time so that the processes involved - fuel-air mixing, ignition and chemical-reaction propagation - can take place to completion. Contours pressure shows the expansion fan around leading edge of injection. There is a recompression shock just near the injection point due to shear layer growth. Figure 4 shows the contours temperature. Contour of static temperature shows the combustion and heat releases to be taking place and the flame spreads upwards as it moves along the wall. Contour of static temperature shows the combustion and heat release to be taking place in the upstream separation region under the adiabatic wall condition because no heat produced by the exothermic reaction is lost through the wall and temperature becomes more than 2500 K. The vicinity of the wall near the small recirculation as well as the downstream region of the injector is filled with unburned fuel gases injected through the injector. The temperature in that region is lower than the injected gas temperature because of under-expansion effects of the injected gas. The high temperature region is located near the upstream boundary of the jet above the small-scale re-circulation rather than at the center region of the small-scale recirculation.

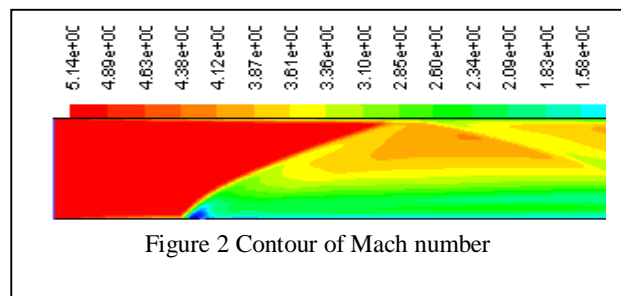


Figure 2 Contour of Mach number

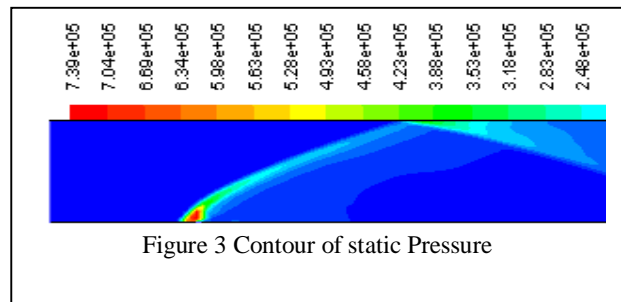


Figure 3 Contour of static Pressure

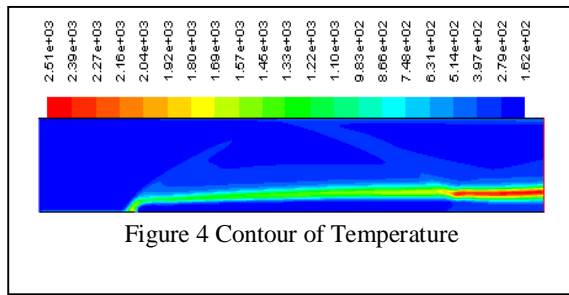


Figure 4 Contour of Temperature

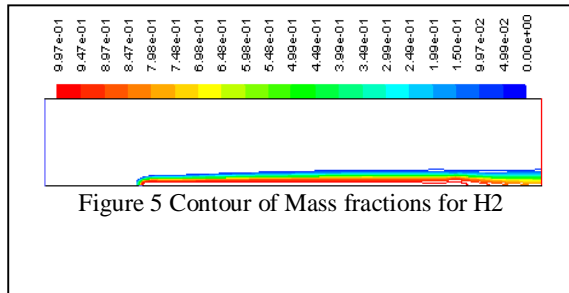


Figure 5 Contour of Mass fractions for H2

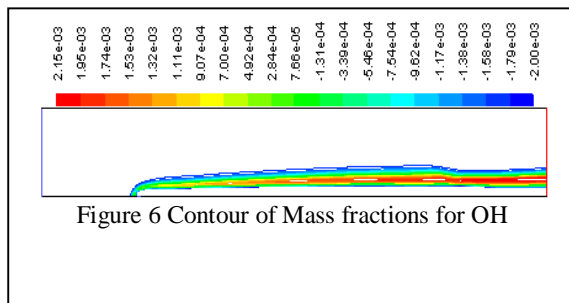


Figure 6 Contour of Mass fractions for OH

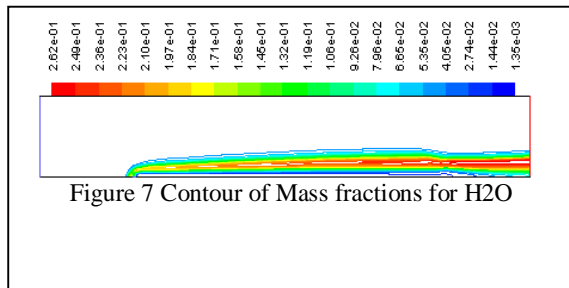


Figure 7 Contour of Mass fractions for H2O

Figure 5, 6 and 7 shows distribution of Hydrogen, OH and mass fraction of water vapour. The mixing becomes more predominant in the region far from the jet outlets and heat release gradually increases in the mixing layer between hydrogen and air. The OH mole fraction is less almost by an order to that of water mole fraction. The OH mass fraction decreases as the gas expands around the injected jet and the local mixture temperature falls. However OH species are primarily produced in the hot separation region upstream of the jet exit and behind the bow shock and convected downstream with shear layer. The OH emission of the flame has been imaged for $57 < x < 300$ m and global visualization allows to estimate the mixing and ignition length of hydrogen within the supersonic flow of air. The water mass fraction values at core region could not be established exactly. Static pressure distribution along the bottom wall for without cavity has been shown in figure 8 and 9 at different x and y location. The initial pressure rise is due to shock wave generated from the downstream region of the injector. There is variation in

pressure at $x=0.058$ m near the injector due to expansion fan while at $x=0.25$ m i.e. near the exit of the combustion chamber, is almost constant while near the upper wall there is little variation in pressure due to bow shock. The static pressure is comparatively high at $x=0.058$ m than $x=0.25$ m, this is because of hydrogen is injected at $x=0.057$ m and from figure 8 it is clearly visualized that there is variation near the lower wall due to recirculation region and barrel shock. The same x-y plot for pressure distribution comes in figure 9 at $y=0.003$ that means near lower wall and $y=0.025$ i.e. in center of the combustion chamber. As it is clear in figure 10 near the injector pressure is high, the same pattern can be seen here in figure 9. Velocity magnitude distribution along the bottom wall for without cavity has been shown in figure 9 and 11 at different x and y location. The variation of velocity magnitude along $x=0.058$ is higher compared to the $x=0.25$ m near the lower wall shown in figure 10, while the velocity magnitude is almost constant in the center of the combustion chamber. There is a lot of variation in velocity magnitude near the injector due to recirculation zone, bow shock and barrel shock in figure 11.

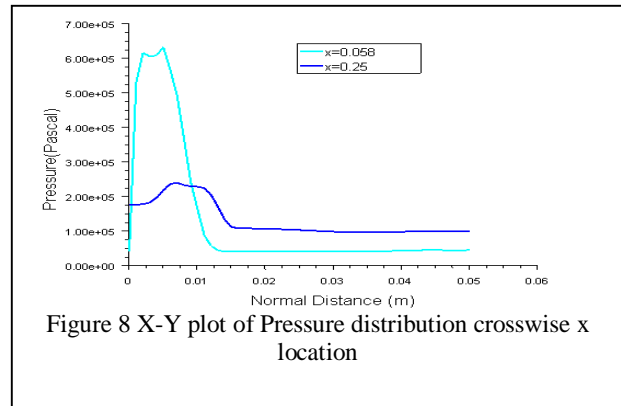


Figure 8 X-Y plot of Pressure distribution crosswise x location

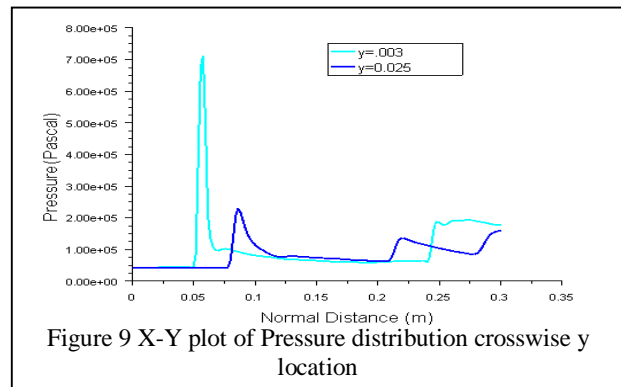


Figure 9 X-Y plot of Pressure distribution crosswise y location

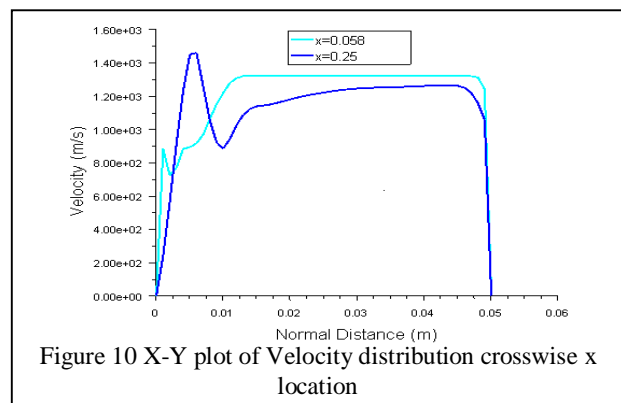


Figure 10 X-Y plot of Velocity distribution crosswise x location

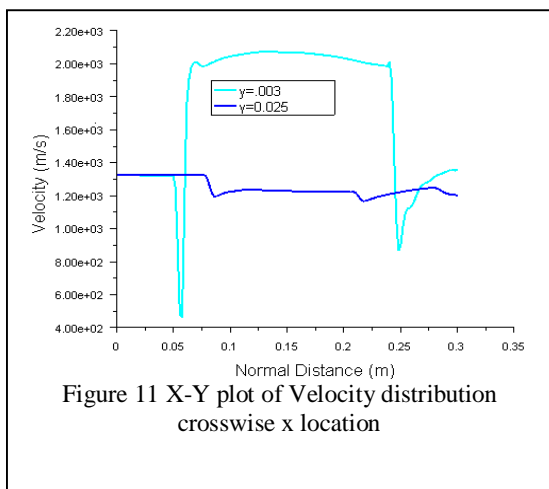


Figure 11 X-Y plot of Velocity distribution crosswise x location

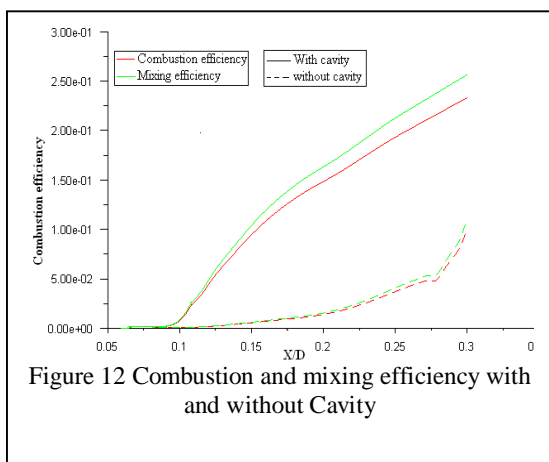


Figure 12 Combustion and mixing efficiency with and without Cavity

The effect of a cavity on mixing and combustion efficiencies is plotted in Figure 12. When the cavity is installed, it is observed in the figure that the combustion as well as mixing efficiency is greatly enhanced, since the mass and thermal transport phenomena are much improved along the shear layer as well as in the cavity. The combustion efficiency is directly related to the total length required for the combustor. The reason is that the higher the combustion efficiency, the shorter the length of combustor becomes. The cavity shape has to be derived from flow stabilization and flame holding requirements.

CONCLUSION

In this, the effect of the cavity on the hydrogen injection in to the supersonic and hypersonic air flow regime has been investigated. The numerical simulation has been done with finite rate chemistry model using K- ϵ turbulence model utilizing CFD Fluent software. Actually the cavity was found to increase both the total pressure loss and the combustion and the temperature of the combustor while enhancing the combustion of the fuel oxidizer. Achieving efficient combustion is very much so dependent on producing homogeneous fuel/air mixture rapidly across the whole combustor. When the offset ratio of upper to downstream depth of the cavity increases, the combustion efficiency as well as the total pressure loss decreases. For higher offset ratio, geometrically the injected gas has expanded more, resulting in reduction in gas temperature so that the chemical

reaction has been retarded. Based on comparison with the case without cavity, a use of cavity is much preferred because cavity the flame temperature is not sufficiently high as in case of with cavity.

REFERENCES

- [1] A. Ben-Yakar And R. K. Hanson, "Experimental Investigation Of Flame-Holding Capability Of Hydrogen Transverse Jet In Supersonic Cross-Flow", Twenty-Seventh Symposium (International) On Combustion/The Combustion Institute, 1998/Pp. 2173-2180,
- [2] A. R. Srikrishnan , J. Kurian And V. Sriramulu "An Experimental Investigation Of Thermal Mixing And Combustion In Supersonic Flows", Combustion And Flame 107:464-474 (1996).
- [3] A.M. Starik, N.S. Titova, L.V. Bezgin, And V.I. Kopchenov, "The Promotion Of Ignition In A Supersonic H₂-Air Mixing Layer By Laser-Induced Excitation Of O₂ Molecules: Numerical Study", Combustion And Flame 156 (2009) 1641-1652.
- [4] B.E. Milton And K. Pianthong, "Pulsed, Supersonic Fuel Jets—A Review Of Their Characteristics And Potential For Fuel Injection", International Journal Of Heat And Fluid Flow 26 (2005) 656-671.
- [5] Chadwick C. Rasmussen, Sulabh K. Dhanuka, And James F. Driscoll, "Visualization Of Flameholding Mechanisms In A Supersonic Combustor Using Plif", Proceedings Of The Combustion Institute 31 (2007) 2505-2512.
- [6] Chadwick C. Rasmussen, James F. Driscoll, Kuang-Yu Hsueh, Jeffrey M. Donbar, Mark R. Gruber, Campbell D. Carter "Stability Limits Of Cavity-Stabilized Flames In Supersonic Flow", Proceedings Of The Combustion Institute 30 (2005) 2825-2833.
- [7] C. Gruenig* And F. Mayinger "Supersonic Combustion Of Kerosene/H₂-Mixtures In A Model Scramjet Combustor", Institute A For Thermodynamics, Technical University Munich, D-85747
- [8] Deepu, Mukundan N., Gokhale, Sadanand. S., jayaraj, Simon, "Numerical Analysis of Supersonic combustion using unstructured Point Implicit finite Volume Method", Journal of combustion Society of Japan, Vol. 48 No. 144(2006) 187-197.
- [9] Doyoung Byun And Seung Wook Baek, "Numerical Investigation Of Combustion With Non-Gray Thermal Radiation And Soot Formation Effect In A Liquid Rocket Engine", International Journal Of Heat And Mass Transfer 50 (2007) 412-422,
- [10] G. Yu, J.G. Li, J.R. Zhao, L.J. Yue, X.Y. Chang, C.-J. Sung "An Experimental Study Of Kerosene Combustion In A Supersonic Model Combustor Using Effervescent Atomization", Proceedings Of The Combustion Institute 30 (2005) 2859-2866,
- [11] H. Mo'Bus, P. Gerlinger, D. Bru'Gemann "Scalar And Joint Scalar-Velocity- Frequency Monte Carlo Pdf Simulation Of Supersonic Combustion" Combustion And Flame 132 (2003) 3-24.
- [12] H. Nagata, M. Sasaki, T. Arai, T. Totani, And I. Kudo, "Evaluation Of Mass Transfer Coefficient And Hydrogen Concentration In Supersonic Flow By Using Catalytic Reaction", Proceedings Of The Combustion Institute, Volume 28, 2000/Pp. 713-719,
- [13] Jean-Francois Izard , Arnaud Mura "Stabilization Of Non-Premixed Flames In Supersonic Reactive Flows" Combustion For Aerospace Propulsion, Cras2b:2818,
- [14] J.X. Wen*, B.P. Xu And V.H.Y. Tam, "Numerical Study On Spontaneous Ignition Of Pressurized Hydrogen Release Through A Length Of Tube", Combustion And Flame 2009.
- [15] Kenji Miki, Joey Schulz, Suresh Menon "Large-Eddy Simulation Of Equilibrium Plasma-Assisted Combustion In Supersonic Flow", Proceedings Of The Combustion Institute 32 (2009) 2413-2420, Atlanta, Ga 30332-0150,
- [16] Kenichi Takita, "Numerical Simulation Of A Counterflow Diffusion Flame In Supersonic Airflow", Twenty-Sixth Symposium (International) On Combustion/The Combustion Institute, 1996/Pp. 2877-2883.
- [17] K. Kumaran, V. Babu "Investigation Of The Effect Of Chemistry Models On The Numerical Predictions Of The Supersonic Combustion Of Hydrogen", Combustion And Flame 156 (2009) 826-841.
- [18] K.M.pandey and A. P. Singh" Transient Analysis of Supersonic Combustion with Jet Co-Flow With Finite Rate Chemistry Model" International Review of Aerospace Engineering, Praise Worthy publications, Vol-4, No.-2, April 2011..
- [19] K.M.pandey and A. P. Singh" Numerical Analysis of Combustor Flow Fields in Supersonic Flow Regime with Spalart-Allmaras And k- ϵ Turbulence Model" International Journal of Engineering and Technology, June 2011, pp.-208-214.
- [20] K.M.pandey and A.P. Singh" Numerical Analysis of Supersonic Combustion by Strut Flat Duct Length with S-A Turbulence Model",

- International Journal Engineering and Technology, April 2011, pp.-193-198.
- [21] K.M. Pandey and A.P Singh, "Numerical Analysis of combustor Flow Fields in Supersonic Flow Regime with Finite Rate Chemistry Model" ISST Journal of Mechanical Engineering, vol.-1, No.2, June- Dec. 2010.
- [22] K.M. Pandey and A.P Singh, "CFD Analysis of Conical Nozzle For Mach 3 At Degrees Of Angle Of Divergence With Fluent Software" International Journal of chemical Engineering and Application ,Vol.-1, No. 2, August 2010,ISSN- 2010-0221, pp 179-185.
- [23] K.M. Pandey and A.P Singh, "Recent Advances in Experimental and Numerical Analysis of Combustor Flow Fields in Supersonic Flow Regime" International Journal of chemical Engineering and Application ,Vol.-1, No. 2, August 2010,ISSN- 2010-0221, pp 132-137.
- [24] K.M. Pandey and A.P Singh, "Design and development of De-Laval Nozzle at Mach 3 and 4 with fluent software" ISST Journal of Mechanical Engineering, vol.-1, No.1, January- June 2010, pp 61-72.
- [25] Kyung Moo Kim 1, Seung Wook Baek *, Cho Young Han " Numerical Study On Supersonic Combustion With Cavity-Based Fuel Injection", International Journal Of Heat And Mass Transfer 47 (2004) 271–286 ,
- [26] Liscinsky, D. S., True, B., and Holdeman, M. A. (1995). "Crossflow mixing of noncircular jets," AIAA Paper 95–0732.
- [27] Peter Gerlinger, Peter Stoll 1, Markus Kindler , Fernando Schneider C, Manfred Aigner "Numerical Investigation Of Mixing And Combustion Enhancement In Supersonic Combustors By Strut Induced Streamwise Vorticity", Aerospace Science And Technology 12 (2008) 159–168.
- [28] P Manna, D Chakraborty "Numerical Simulation of Transverse H2 Combustion In Supersonic Airstream In A Constant Area Duct", Vol. 86, November 2005, ARTFC.
- [29] P.K. Tretyakov "The Problems Of Combustion At Supersonic Flow" West-East High Speed Flow Field Conference 19-22, November 2007.
- [30] Poinso, T. and Veynante, D. (2005). Theoretical and Numerical Combustion, 2nd ed., R. T. Edwards, Inc.
- [31] S. Javoy , V. Naudet , S. Abid , C.E. Paillard, "Elementary Reaction Kinetics Studies Of Interest In H2 Supersonic Combustion Chemistry", Experimental Thermal And Fluid Science 27 (2003) 371–377.
- [32] Shigeru Aso, Arifnur Hakim, Shingo Miyamoto, Kei Inoue And Yasuhiro Tani " Fundamental Study Of Supersonic Combustion In Pure Air Flow With Use Of Shock Tunnel" , Acta Astronautica 57 (2005) 384 – 389.
- [33] T. Cain And C. Walton "Review Of Experiments On Ignition And Flame Holding In Supersonic Flow" Published By The America Institute Of Aeronautics And Astronautics, Rto-Tr-Avt-007-V2.
- [34] Yakhot, V., Orzag, A., Gatski, T. B., and Speziade, C. B, Physics of Fluids, 4: 1510-1520 (1992).
- [35] Yuan Shengxue, "On Supersonic Combustion", Voi. 42 No. 2, Science In China (Series A) February 1999.
- [36] Zhiliang Xuxk, Myoungnyoun Kimxk, Wonho Ohzk, James Glimmzkk, Roman Samulyakx, Xiaolin Liz And Constantine Tzanos "Atomization Of A High Speed Jet" April 14, 2005, U.S. Department Of Energy
- [37] Zheng Chen, Xiao Qin, Yiguang Ju *, Zhenwei Zhao, Marcos Chaos, Frederick L. Dryer, "High Temperature Ignition And Combustion Enhancement By Dimethyl Ether Addition To Methane–Air Mixtures", Proceedings Of The Combustion Institute 31 (2007) 1215–122.